

Particle energy cascade in the intergalactic medium

M. Valdés¹, C. Evoli² and A. Ferrara³

¹ IPMU, University of Tokyo, 5-1-5 Kashiwanoha, Kashiwa, Chiba 277-8568, Japan

² SISSA/ISAS, via Beirut 2-4, 34151 Trieste, Italy

³ Scuola Normale Superiore, Piazza dei Cavalieri 7, 56126 Pisa, Italy

13 February 2022

ABSTRACT

We study the development of high energy ($E_{\text{in}} \leq 1$ TeV) cascades produced by a primary electron of energy E_{in} injected into the intergalactic medium (IGM). To this aim we have developed the new code MEDEA (Monte Carlo Energy DEposition Analysis) which includes Bremsstrahlung and Inverse Compton (IC) processes, along with H/He collisional ionizations and excitations, and electron-electron collisions. The cascade energy partition into heating, excitations and ionizations depends primarily on the IGM ionized fraction, x_e , but also on redshift, z , due to IC on CMB photons. While Bremsstrahlung is unimportant under most conditions, IC becomes largely dominant at energies $E_{\text{in}} \geq 1$ MeV. The main effect of IC at injection energies $E_{\text{in}} \leq 100$ MeV is a significant boost of the fraction of energy converted into low energy photons ($h\nu < 10.2$ eV) which do not further interact with the IGM. For energies $E_{\text{in}} \geq 1$ GeV CMB photons are preferentially upscattered within the X-ray spectrum ($h\nu > 10^4$ eV) and can free stream to the observer. Complete tables of the fractional energy depositions as a function of redshift, E_{in} and ionized fraction are given. Our results can be used in many astrophysical contexts, with an obvious application related to the study of decaying/annihilating Dark Matter (DM) candidates in the high- z Universe.

Key words: intergalactic medium - cosmology: theory - diffuse radiation - dark matter

1 INTRODUCTION

High energy particles can be produced by several astrophysical and cosmological sources through different acceleration processes. The energy stored in relativistic particles might be a non-negligible fraction of the total energy of these systems and therefore an obvious question arises about how this energy is eventually thermalized and transferred to the surrounding environment. In spite of its importance, this question has received only a relatively limited attention. Previous works have considered non-relativistic initial energies of up to 10 keV (e.g. Shull 1979, Shull & van Steenberg 1985, Dalgarno et al. 1999; Valdés & Ferrara 2008, hereafter VF08; Furlanetto & Johnson Stoever 2009). In this energy range processes such as free-free emission with charged particles and Inverse Compton (IC) with a diffuse distribution of photons can be safely neglected.

However for many astrophysical applications it is necessary to deal with higher energy particles: extrapolating the results and fitting formulae presented in the aforementioned works can lead to substantially incorrect results. Particles can be accelerated to relativistic energies in a number of astrophysical systems, leading to the emission of synchrotron and Compton radiation observable in a broad range of en-

ergy bands. Active Galactic Nuclei, Stellar flares, Gamma Ray Bursts, Pulsar Wind Nebulae, Supernova Remnants are believed to house a population of shock accelerated electrons (see e.g. MacKinnon & Mallik 2009; Venter & de Jager 2008; Resmi & Bhattacharya 2008). It is then important to consider extensions of these works to compute at best the evolution of the energy cascade of relativistic electrons of energy E_{in} into a partially ionized gas under realistic cosmological conditions including the presence of CMB photons.

Radio observations of galaxy clusters have revealed the existence of the so-called radio "relics" which can be explained with the presence in the intracluster medium of relativistic electrons accelerated by shocks due to cluster merging. This can give rise to X-ray emission through IC of CMB photons, as recent observations of the satellites Beppo-SAX and RXTE seem to indicate (see e.g. Rephaeli 1977; Fusco-Femiano, Landi, & Orlandini 2007; Rephaeli et al. 2008; Ferrari 2009).

Another astrophysical source of relativistic electrons could come from the decay or annihilation of DM particles. If indeed, as many theoretical models predict, this elusive matter component of the Universe injects relativistic electrons and positrons into the IGM and the consequent inverse Compton scattering with the CMB photons could generate a

2 Valdés, Evoli & Ferrara

distortion of the black body spectrum by Sunyaev-Zeldovich (SZ) effect (see e.g. Lavalle, Boehm, & Barthes 2009; Colafrancesco & Mele 2001; Colafrancesco 2004; Colafrancesco, Profumo, & Ullio 2006). In the near future the recently launched satellite Planck (The Planck collaboration, 2006) and the ALMA array (Wootten & Thomson 2009) could detect the SZ deviation induced by DM decays/annihilations.

In the past few years a large number of works has investigated the effects and detectability of DM decays/annihilations into the high redshift IGM via observations of the redshifted 21 cm hyperfine triplet-singlet level transition of the ground state of neutral hydrogen (Shchekinov & Vasiliev 2006; Furlanetto, Oh, & Pierpaoli 2006; Valdés et al. 2007; Natarajan & Schwarz 2009). The interest for such kind of studies is generated by the present or planned construction of large radio interferometers such as the Low frequency Array (LOFAR, <http://www.lofar.org/>), the 21 Centimeter Array (21CMA, <http://21cma.bao.ac.cn/>), the Murchison Widefield Array (MWA, <http://www.mwatelescope.org/>) and the Square Kilometer Array (SKA, <http://www.skatelescope.org/>). These instruments will in fact open a new observational window by the detection of the HI 21 cm line at $z > 6$ (e.g. Peterson, Pen & Wu 2005; Bowman, Morales, & Hewitt 2005; Kassim et al. 2004; Wyithe, Loeb, & Barnes 2005).

To understand if observations of the redshifted HI 21 cm line can help constrain DM it is crucial to follow in detail the energy cascade from energetic primary photons or electrons up to energies much higher than previously studied (Shull & van Steenberg 1985, VF08) to include those DM candidates that can produce relativistic electrons. In our calculations we choose an initial electron energy $1 \text{ MeV} < E_{\text{in}} < 1 \text{ TeV}$. The details of the energy degradation of electrons in this energy range are of great interest for many of the aforementioned astrophysical sources and in particular for the study of the effects of DM decays/annihilations, since recent data from PAMELA, ATIC, FERMI-LAT and HESS experiments have shown that there are electron-positron excesses in the cosmic ray energy spectrum which can be explained by annihilations of DM between 1 to 2 TeV (see e.g. Cirelli, Franceschini, & Strumia 2008; Liu et al. 2009; Berg et al. 2009; Hooper & Tait 2009; Chen, Takahashi & Yanagida 2009; He 2009 for a brief review with an extensive list of citations). Recently Slatyer et al. (2009) computed the energy injection rates for some annihilating DM candidates.

The rest of the paper is organized as follows. In Sec. 2 we describe the relevant physical process and their implementation into the multi-purpose code MEDEA (Monte Carlo Energy DEposition Analysis) we have developed to follow the energy cascade. In Sec. 3 we present the results and analyze their dependence on redshift, initial electron energy and redshift. In Sec. 4 we discuss the implications and draw some conclusions. The complete numerical outputs of MEDEA can be found in tabulated form in Appendix A.

2 METHOD

Our code MEDEA, a substantial extension of the algorithm described in VF08, is based on a Monte Carlo scheme that allows to follow the energy cascade arising from the interac-

tion of relativistic electrons ($1 \text{ MeV} < E_{\text{in}} < 1 \text{ TeV}$) with the IGM for $10 < z < 50$.

A Monte Carlo method is a computational algorithm that relies on repeated random sampling of the relevant physical quantities and processes (e.g. cross-sections and interaction probabilities) to follow the evolution of the system. Essentially the code calculates for every particle the probability of the main interaction channels and then selects one by a random number generator. Once the reaction happens the code follows the resulting particles to the next interaction, until the energy of the particle drops below a given threshold taken in our case to be 10.2 eV (the Lyman α transition energy), when the photon-gas interaction rate vanishes (in the absence of heavy elements, molecules or dust).

For each assumed primary energy E_{in} , gas ionized fraction x_e , and redshift, z , we performed 100 Monte Carlo realizations. Although in VF08 we performed 1000 realizations for each parameter choice, the full MEDEA proved to be very computationally expensive since the large energies considered imply a much more complex cascade. In particular, IC interactions with the CMB required the code to follow in detail a large amount of upscattered photons. In VF08 we found that while 1000 Monte Carlo realizations gave highly consistent results, going from 1000 to 50 realizations changed the averaged values by less than 5% and the respective σ by less than 10%. Therefore performing 100 realization per parameter choice does not bring any substantial bias due to the random nature of the computation.

In this Section the physics related to the low energy processes $E_{\text{in}} \leq 10^4 \text{ eV}$ will be reviewed briefly and defer the reader to VF08 for details. We will instead describe extensively the implementation of the two newly included high energy processes, Bremsstrahlung and Inverse Compton, which were previously not included or negligible.

2.1 Low energy regime

MEDEA follows in detail the fate of relativistic electrons by calculating the energy cascade that originates from a number of interactions with the surrounding gas. When a secondary electron or photon of energy below 10 keV is produced the code behaves consistently to the calculation described in VF08. An ionizing photon of energy $h\nu < 10 \text{ keV}$ will be immediately converted into an electron since the dominant interaction in this case is photoionization of an H or He atom (see e.g. Zdziarski & Svensson 1989). Then the code follows the fate of each of these electrons by calculating the mean free paths relative to a number of possible interactions: H, He, HeI collisional ionizations; H, He collisional excitations; collisions with thermal electrons; free-free interactions with ionized atoms; recombinations. The latter two are virtually negligible as stated in VF08. We assume that $x_e \equiv n(\text{H}^+)/n(\text{H}) \equiv n(\text{He}^+)/n(\text{He})$ and that the helium fraction by mass is $f_{\text{He}} = 0.248$ in agreement with the 3-yr Wilkinson Microwave Anisotropy Probe (WMAP) data analysis (Spergel et al. 2007).

Every collisional ionization event by an electron with an H or He atom generates another free electron whose further interactions with the gas will be followed in detail by the code. These energy ramifications find an end when secondary electron energies drops below 10.2 eV and their entire energy

is subsequently deposited as heat by thermalization with gas. This is a good assumption at the redshifts of interest and in general for a gas with a temperature below 10^4 K. The energy distribution of electrons generated after collisional ionization of H and He are treated as in VF08.

We also follow individual photons emitted by excited atoms returning to the ground state after a collision with a free electron. Photons with energies lower than 10.2 eV do not interact further with the gas while higher energy photons do and are followed by the code. As in VF08 also transitions to/from the 2s level of HI are considered, i.e. direct collisional excitations to 2s followed by the two-photon forbidden transition $2s \rightarrow 1s$ or indirect cascades from $n \geq 3$ states which happen preferentially through the 2s level rather than through 2p (see e.g. Hirata 2006, Chuzhoy & Shapiro 2007).

Electron-electron collisional cross section resulting in an energy loss ΔE_{in} is given by:

$$\sigma_{ee} = 40\pi e^4 \ln \Lambda \left(\frac{0.05}{f} \right) E_{\text{in}}^{-2} \text{ cm}^2 \quad (1)$$

where the Coulomb logarithm $\ln \Lambda = \ln(4E_{\text{in}}/\zeta_e)$ with $\zeta_e = 7.40 \times 10^{-11} (n_e/\text{cm}^{-3})$ eV (Furlanetto & Johnson Stoever 2009) and $f = \Delta E_{\text{in}}/E_{\text{in}} = 0.05$ is chosen to account for the discrete nature of the calculation. This process is now implemented with higher accuracy with respect to VF08 and this eliminates the discrepancy in the heating fractional energy deposition f_h at moderate and high ionized fractions observed by Furlanetto & Johnson Stoever (2009).

After Coulomb scattering events kinetic energy is transferred elastically to the thermal electrons present in the IGM and our code follows consistently the fate of the upscattered electrons.

We report here briefly the references for the cross sections used to account for the several processes considered: (i) collisional ionization of H, He, He+ were taken from Kim & Rudd (1994), Shah et al. (1987), Shah et al. (1988); collisional excitation cross sections of H and He are from Stone, Kim & Desclaux (2002); collisional excitation cross section to the 2s level of H is from Bransden & Noble (1976); cross section for Coulomb collisions between electrons is from Spitzer & Scott (1969).

The hydrogen recombination cross section is given by

$$\sigma_r(\nu, n) \approx 3 \times 10^{10} \frac{g_{\text{fb}}}{\nu n^3 v_e^2} \text{ cm}^2 \quad (2)$$

where g_{fb} is the Gaunt factor of $\mathcal{O}(1)$, calculated and tabulated by Karzas & Latter (1961), ν is the emitted radiation frequency, v_e is the electron velocity and n is the level at which the electron recombines.

2.2 Bremsstrahlung

In a free-free (or Bremsstrahlung) interaction between an electrons with either a proton, ionized He atom or neutral H and He atoms the electron decelerates and therefore a continuum photon is emitted. This process has been studied in great detail by several groups and the theoretical and experimental results gathered are assembled in a few review works (see e.g. Koch & Motz 1959, Blumenthal & Gould 1970) where analytical cross section formulae are given for a number of different conditions and approximations.

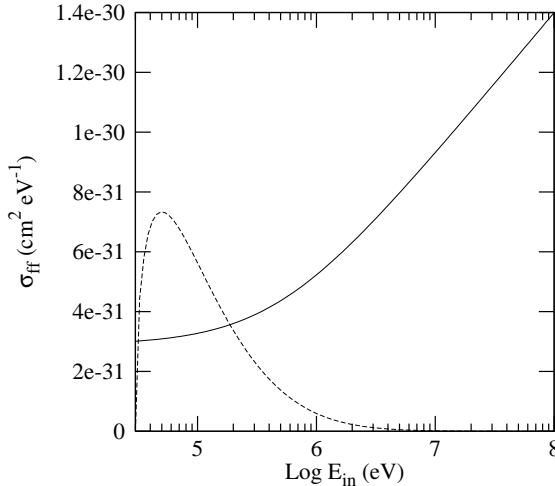


Figure 1. Cross section for Bremsstrahlung leading to the emission of a 30 keV photon as a function of the initial electron kinetic energy. The two curves represent the non-relativistic (dashed line) and relativistic limit (solid line).

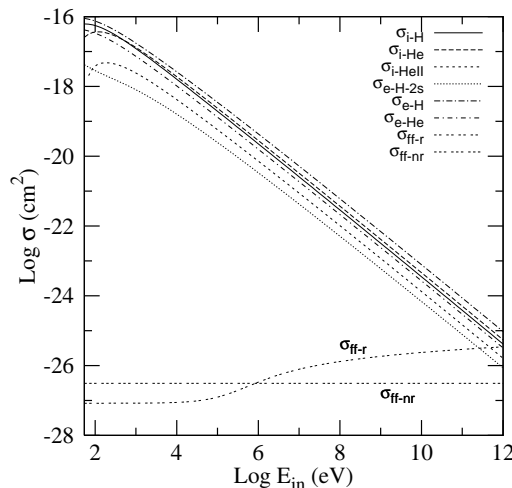


Figure 2. Comparison between interactions included in MEDEA. The labels within the plot box from top to bottom stand respectively for the following cross sections: H ionization; He ionization; HeII ionization; H excitation to the 2s level; H excitation; He excitation; relativistic free-free; non-relativistic free-free.

In general the exact Bremsstrahlung cross sections can be derived by the methods of quantum electrodynamics but it is possible to make reasonable assumptions and simplifications to obtain approximated cross sections by a semiclassical approach. We refer the reader to the aforementioned references for details on the approximated cross sections.

The two main regimes to consider are the relativistic and non-relativistic one. In Fig 1 we show the cross section for electron-proton Bremsstrahlung leading to the emission of a 30 keV photon as a function of the initial electron kinetic energy in the non-relativistic and relativistic limits. Bremsstrahlung can also take place between free electrons and atoms, in which case screening by atomic electrons has to be taken into account in the calculations.

We include in our calculation two different cross sections for the non-relativistic and relativistic case. We find that for

most of the considered energy range Bremsstrahlung is negligible in comparison to other processes. This can be seen clearly in Fig 2 which represent a direct comparison of the cross sections of the several processes included in MEDEA. We do not include inverse Compton in the plot since it is related to CMB photons and it is therefore not visually comparable to the other interactions. The two curves labeled $\sigma_{\text{ff}-\text{nr}}$ and $\sigma_{\text{ff}-r}$ in the plot are the total radiation cross section derived by the Born approximation procedure for the cases:

- Non-relativistic; not screened
- Relativistic; not screened

respectively. Only for values $E_{\text{in}} \geq 10^{11}$ eV $\sigma_{\text{ff}-r}$ becomes comparable to the other cross sections reported.

2.3 High energy regime: Inverse Compton

When electron energies become relativistic Inverse Compton with CMB photons becomes by far dominant. To understand why we first introduce briefly the physics of this particular process. The following is the inverse Compton angle averaged cross section in $\text{cm}^{-2} \text{eV}^{-1}$.

$$\sigma_{\text{KN}}(E_{\text{in}}^{\gamma}, E_{\text{fin}}^{\gamma}, \gamma_e) = \frac{3\sigma_T}{4\gamma_e^2 E_{\text{in}}^{\gamma}} G(q, \eta). \quad (3)$$

We denote here by E_{in}^{γ} , E_{fin}^{γ} and γ_e the energy of the incoming and outgoing photon and the Lorentz factor of the incoming electron, respectively. $\sigma_T = 8\pi r_0^2/3$ is the Thomson cross-section while the function $G(q, \eta)$ is given by:

$$G(q, \eta) = 2q \ln q + (1+2q)(1-q) + 2\eta q(1-q), \quad (4)$$

$$q = \frac{E_{\text{fin}}^{\gamma}}{\Gamma(\gamma_e m_e c^2 - E_{\text{fin}}^{\gamma})}, \quad \Gamma = \frac{4E_{\text{in}}^{\gamma} \gamma_e}{m_e c^2}, \quad \eta = \frac{E_{\text{in}}^{\gamma} E_{\text{fin}}^{\gamma}}{(m_e c^2)^2}. \quad (5)$$

The energy distribution of the scattered photons is:

$$\begin{aligned} \frac{dN_{\gamma, E_{\text{in}}^{\gamma}}}{dt dE_{\text{fin}}^{\gamma}} &= \frac{2\pi r_0^2 c}{\gamma_e^2} \frac{n(E_{\text{in}}^{\gamma}) dE_{\text{in}}^{\gamma}}{E_{\text{in}}^{\gamma}} G(q, \eta) = \\ &= c \sigma_{\text{KN}} n(E_{\text{in}}^{\gamma}) dE_{\text{in}}^{\gamma}. \end{aligned} \quad (6)$$

The only assumption for the validity of these equations is that $\gamma_e \gg 1$, i.e. that the electron is relativistic. If the energy of the incoming photon in the rest frame of the electron $E_{\text{in}}^{\gamma *} = \gamma_e E_{\text{in}}^{\gamma} (1 - \beta \cos \theta) \ll m_e c^2$ we are in the Thomson limit, therefore $\Gamma \ll 1$ and the last term in $G(q, \eta)$ becomes negligible. The opposite case $E_{\text{in}}^{\gamma *} \gg m_e c^2$ is the extreme Klein-Nishina limit. If we consider a CMB photon at $z \sim 10$ ($E_{\text{in}}^{\gamma} \sim 2.35 \times 10^{-3}$ eV) and electron energies up to 1 TeV ($\gamma_e \sim 10^6$) we are still well within the Thomson limit; we will therefore assume that scatterings happen in this regime throughout the rest of this work. Kinematic requirements in the Thomson limit set a lower and upper limit on the energy of the up-scattered CMB photon (see e.g. Blumenthal & Gould 1970; Petruk 2009):

$$E_{\text{fin}(\min)}^{\gamma} = E_{\text{in}}^{\gamma}, \quad E_{\text{fin}(\max)}^{\gamma} = 4\gamma_e^2 E_{\text{in}}^{\gamma} \quad (7)$$

For our purposes we consider $\sigma_{\text{KN}}(E_{\text{in}}^{\gamma}, E_{\text{fin}}^{\gamma}, \gamma_e)$ which is given in $\text{cm}^2 \text{eV}^{-1}$: from this quantity we can derive the total inverse-Compton cross-section for an electron and a photon with assigned initial energies by integrating eq. (2) on the energy of the outgoing photon,

$$\sigma_{\text{IC}}(E_{\text{in}}^{\gamma}, \gamma_e) = \int_{E_{\text{in}}^{\gamma}}^{4\gamma_e^2 E_{\text{in}}^{\gamma}} dE_{\text{fin}}^{\gamma} \frac{3\sigma_T}{4\gamma_e^2 E_{\text{in}}^{\gamma}} G(E_{\text{fin}}^{\gamma}). \quad (8)$$

We can now derive the probability for a given high energy electron to scatter off CMB photons described by the distribution $n(E_{\text{in}}^{\gamma})$. As in VF08 we compute the mean free path for inverse Compton to compare it with those from the other processes. We have that, for the generic i -th process, $\lambda_i = 1/\sigma_i n_i$, therefore:

$$\lambda_{\text{IC}}(\gamma_e) = \frac{1}{\int dE_{\text{in}}^{\gamma} n(E_{\text{in}}^{\gamma}) \sigma_{\text{IC}}(E_{\text{in}}^{\gamma}, \gamma_e)}. \quad (9)$$

This quantity is dependent only on the initial electron energy if the isotropic initial photon energy distribution is known. Now we can calculate the relative probability of having inverse Compton and can follow the route of the electron into the IGM by Monte Carlo technique.

If the electron actually scatters off a CMB photon we need to compute the energy kick to the photon and therefore the energy loss of the electron. To do so we have to determine first which is the initial photon energy since we computed the mean free path in a distribution of photons. For this purpose we have to use the rejection method to generate sampling photons from the distribution given by $n(E_{\text{in}}^{\gamma}) \cdot \sigma_{\text{IC}}(E_{\text{in}}^{\gamma}, \gamma_e)$.

Once we determine E_{in}^{γ} we can use similarly the rejection method on the distribution $\sigma_{\text{KN}}(E_{\text{in}}^{\gamma}, E_{\text{fin}}^{\gamma}, \gamma_e)$ to infer the outgoing photon energy - and therefore the electron's energy loss.

Because we operate in the Thomson limit the mean free path of an electron in a photon background is very well approximated by:

$$\lambda_{\text{IC}} = \frac{1}{\sigma_T \int dE_{\text{in}}^{\gamma} n(E_{\text{in}}^{\gamma})}. \quad (10)$$

Inverse Compton is by far the process that requires the higher computational effort when following the cascade evolution since (i) it is the most probable interaction for a wide range of energies and (ii) energy loss by upscattering of CMB photons generally happens thorough a very high number of interactions that lower the electron kinetic energy by a small fraction at each step, accordingly to the limits given by Eq. (7).

In agreement with the analytical comparison between the collisional ionization process and inverse Compton by Hansen & Haiman (2004) we find that the latter is the dominant energy loss process at energies

$$E_{\text{in}} = \gamma_e m_e c^2 > \left(\frac{1+z}{21} \right)^{-1/2} \text{MeV}. \quad (11)$$

3 RESULTS

We present our results in Figs. 3-6 and report the tabulated fractional energy depositions in Appendix A, Tables A1-A21, for $z = 10, 30, 50$, for values of the ionized fraction x_e regularly spaced in log-scale with values ranging from 10^{-4} to 0.99 and for energies between 1 MeV and 1 TeV. The columns indicate, from left to right, which fraction of the initial electron energy is deposited into heat, Ly α excitations, ionizations, photons with $E < 10.2$ eV, photons with $E > 10^4$ eV and the total energy of CMB photons before they are upscattered. Hereafter we will refer to these

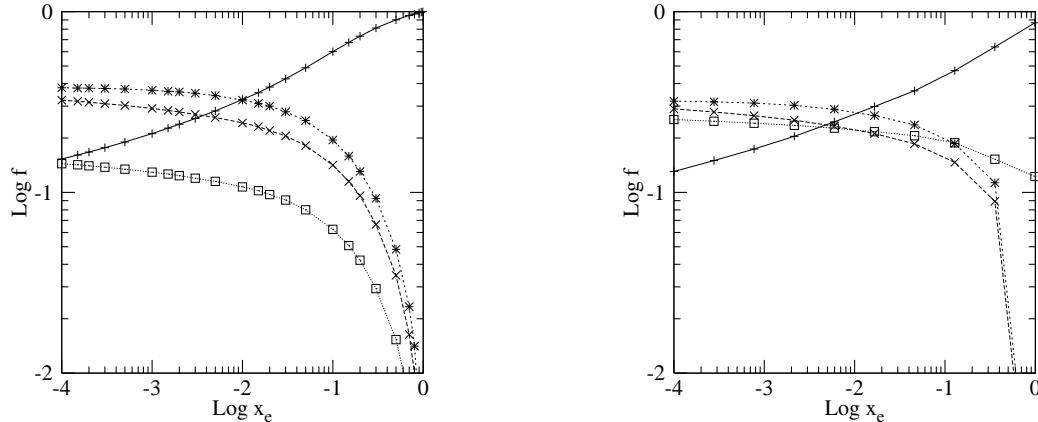


Figure 3. Left panel: Fractional energy losses for a primary 10 keV electron. The data points stand for: photons with $E < 10.2\text{ eV}$ (squares); gas heating (pluses); Ly α photons (crosses), and ionizations (asterisks). The calculation is performed for 25 values of x_e chosen between $x_e = 0.0001$ and $x_e = 0.99$. Right: Same for the case of a 1 MeV primary electron. The fractional energy depositions in this case are calculated for 9 values of x_e chosen between $x_e = 0.0001$ and $x_e = 0.99$.

values as f_h , f_a , f_i , f_c , f_{HE} and f_{CMB} respectively. The latter column is just a test required to ensure that energy is conserved.

The results, consistently with VF08, depend on the ionized fraction x_e which remains the most important parameter for the calculations. We also find a less marked dependence on z due to the implementation in MEDEA of IC interactions with CMB photons.

In Fig 3 we show the differences between the 10 keV results described in VF08 and the lowest energy case considered here, $E_{\text{in}} = 1 \text{ MeV}$. Notice that in the latter we perform the calculation for only 9 different choices of x_e because of the higher computational burden required by running MEDEA. The considered redshift is $z = 10$. While f_i , f_a and f_h appear to have similar behaviors in the two cases it is evident that f_c is increased in the 1 MeV plot. The reason for this is the inclusion of IC: even at relatively low energies in fact IC cross section is dominating. The range of energies of the upscattered CMB photons is however very narrow (see eq. 7) and therefore individual events will enhance the photon energy to values $0.00259 \text{ eV} \leq h\nu \leq 0.0905 \text{ eV}$. We assumed here for simplicity that the CMB photon is at the mean CMB energy at $z = 10$ but in the code we include the proper CMB spectral distribution.

So many CMB photons are upscattered that even though the energy injection from the electrons is small the overall effect is still a significant increase of f_c , by a factor ~ 2 for low values of x_e and by over an order of magnitude for $x_e = 0.99$. The reason for the different rise of the curve for low and high values of x_e is simply that IC is not affected by x_e , therefore the curve increases by a fixed value ~ 0.12 with respect to the 10 keV case.

When the primary electron energy is degraded by the numerous IC scatterings to values below 10 keV then the secondary cascade behaves consistently with the results shown in the left panel of Fig.3 and therefore the fractional energy depositions with the exception of f_c retain the same ratios relative to each other.

Notice that the process other than IC that produces continuum photons at energies lower than 10.2 eV is, as mentioned earlier, the two photon forbidden transition $2s \rightarrow$

1s which we included in VF08 and that was neglected in previous studies (e.g. Shull & van Steenberg 1985).

We focus now on the higher energy results presented in Fig 4. Here the panels show the fractional energy depositions for energies 10 MeV (top left panel), 100 MeV (top right), 1 GeV (bottom left) and 1 TeV (bottom right). Two new kinds of data points appear in some of the panels: the filled squares represent the fraction of the total energy that is deposited into high energy electrons with $h\nu > 10^4 \text{ eV}$ (f_{HE}) while the circles show the integrated energy of CMB photons involved in an IC scatter (f_{CMB}), before they are actually scattered. We keep track of the latter for an energy conservation sanity check.

When a photon is upscattered by IC there are four main energy ranges that we treat differently. Photons with energies below 10.2 eV are added to f_c ; the rare photons with energies between 10.2 eV and 13.6 eV (which we denote as Lyman-continuum photons) are converted into Ly α photons (therefore increasing f_a) while the difference in energy is added to f_c ; photons with $13.6 \text{ eV} \leq h\nu \leq 10^4 \text{ eV}$ are assumed to ionize an atom and are converted into free electrons which we keep following in detail; photons with $h\nu > 10^4 \text{ eV}$ instead stream into the IGM and are added up to the fraction f_{HE} (see e.g. Zdziarski & Svensson 1989; Slatyer et al. 2009). Obviously the range of energies will depend on the energy of the primary electron, as the maximum energy of the upscattered photon is proportional to the square of the Lorentz factor or the electron γ_e .

The differences that we identified when going from the 10 keV to the 1 MeV case are sharply enhanced if we consider a higher initial electron energy $E_{\text{in}} = 10 \text{ MeV}$. Inverse Compton remains in fact dominant but the maximum energy that the electron can give to an average $z = 10$ CMB photon is now of the order of 5 eV. This means that there is a dramatic boost in the fractional deposition f_c , which reaches an almost constant value of ~ 0.8 . The other fractional energy curves are left unchanged relative to each other except for f_a which is raised by some CMB photons with higher than average energy that are upscattered to Lyman-continuum values.

The 100 MeV panel shows curves with very similar

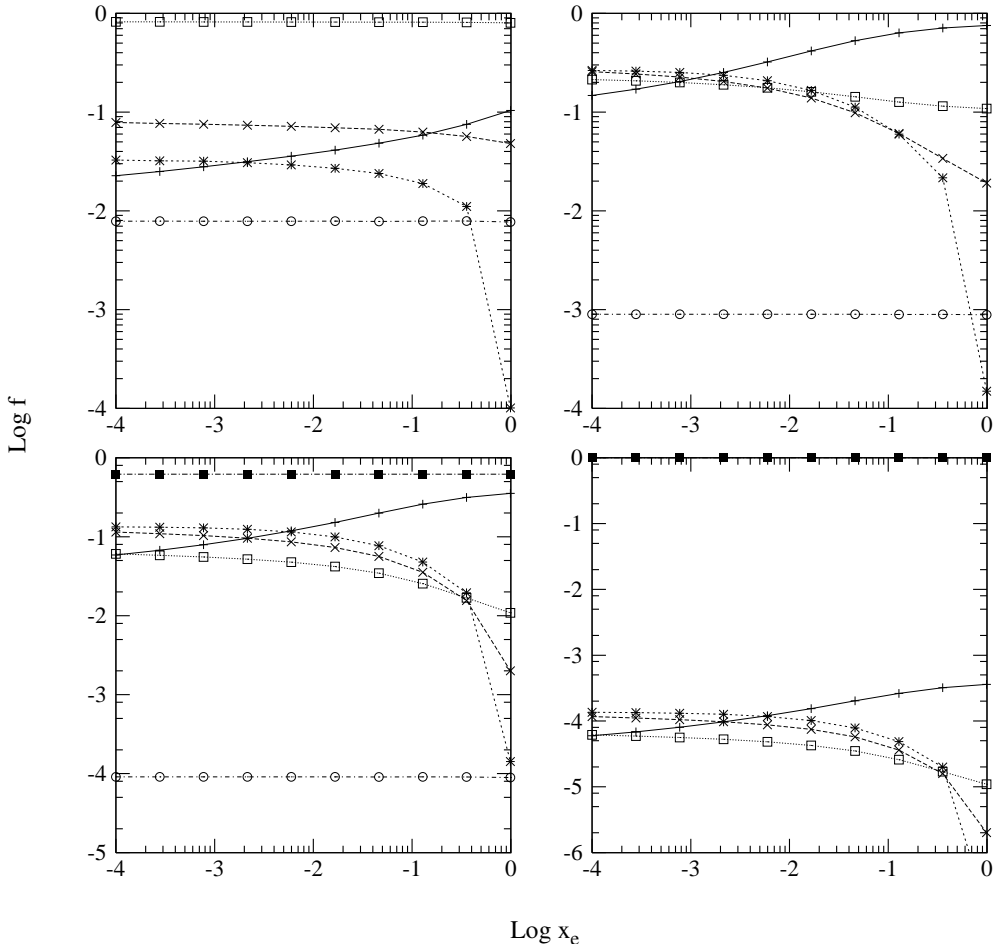


Figure 4. Fractional energy losses for a primary electron of energy 10 MeV, 100 MeV, 1 GeV, 1 TeV, left to right, top to bottom panels. The data points stand for: photons with $E < 10.2\text{ eV}$ (squares); gas heating (pluses); Ly α photons (crosses); ionizations (asterisks); high energy photons with $h\nu > 10^4 \text{ eV}$ (filled squares); energy of upscattered CMB photons (circles).

properties to the 1 MeV case. The reason for this is that now IC can upscatter photons up to values of a few hundred of eV, which ionize atoms, are converted into electrons and behave, consistently with VF08, as in the left panel of Fig.3.

A major difference in behavior is reported in the panel corresponding to 1 GeV. For such high energy primary electrons the IC scattering events preferentially increase CMB photon energies to values $h\nu > 10 \text{ keV}$. In this case the f_{HE} curve makes its first appearance and is already dominant, with a very flat behavior with value ~ 0.61 . The other curves are left practically unchanged relative to each other, but are lowered to $\sim 30\%$ of the values calculated for the 10 keV case.

Finally the last panel reports the curves for a 1 TeV primary electron. For such a high initial energy $f_{\text{HE}}=0.99$ is entirely dominant, while the other fractional energy depositions are reduced to around 1% of the 1 MeV values. Even in this case the amount of E_{in} that goes into ionizations, excitations and heating is hardly negligible: for a 1 TeV electron there is still a total energy of $\sim 10^{-4} \times 10^{12} = 100 \text{ MeV}$ that is injected into the surrounding gas.

In Fig 5 we plot the fractional energy depositions (same symbols correspond to the same quantities as in Fig 4) but

as a function of the initial electron kinetic energy and for fixed values of the ionized fraction, $x_e = 1.000 \cdot 10^{-4}, 2.147 \cdot 10^{-3}, 4.610 \cdot 10^{-2}, 9.900 \cdot 10^{-1}$ for panels left to right top to bottom. Redshift is fixed at $z = 10$.

In the panels it is possible to identify the effects of IC at different energies. For instance the bump in f_c for primary electron energy 10^7 eV is clearly visible in all the panels. The sharp decrease of f_{CMB} is due to the fact that as electrons become relativistic IC encounters upscatter CMB photons to high energies. Therefore the electron will need less interactions to loose its kinetic energy.

On the other hand at around 1 GeV there is a sharp increase in the IC high energy photons and therefore the other curves will decrease accordingly. At 1 TeV $f_{\text{HE}} \sim 1$.

Fig 6 is a summary of our results as it reports the iso-contour plot of the fractional energy depositions as a function of both the ionized fraction x_e and the initial electron energy E_{in} . One interesting feature is visible in the panels relative to the fractional energy that goes into ionizations, f_i . At $z = 10$ there is a clear double peak, with the values decreasing sharply for $E_{\text{in}} \sim 10 \text{ MeV}$. This is a behavior that we reported as we commented the first panel in Fig. 4 corresponding to an initial energy of 10 MeV: IC is al-

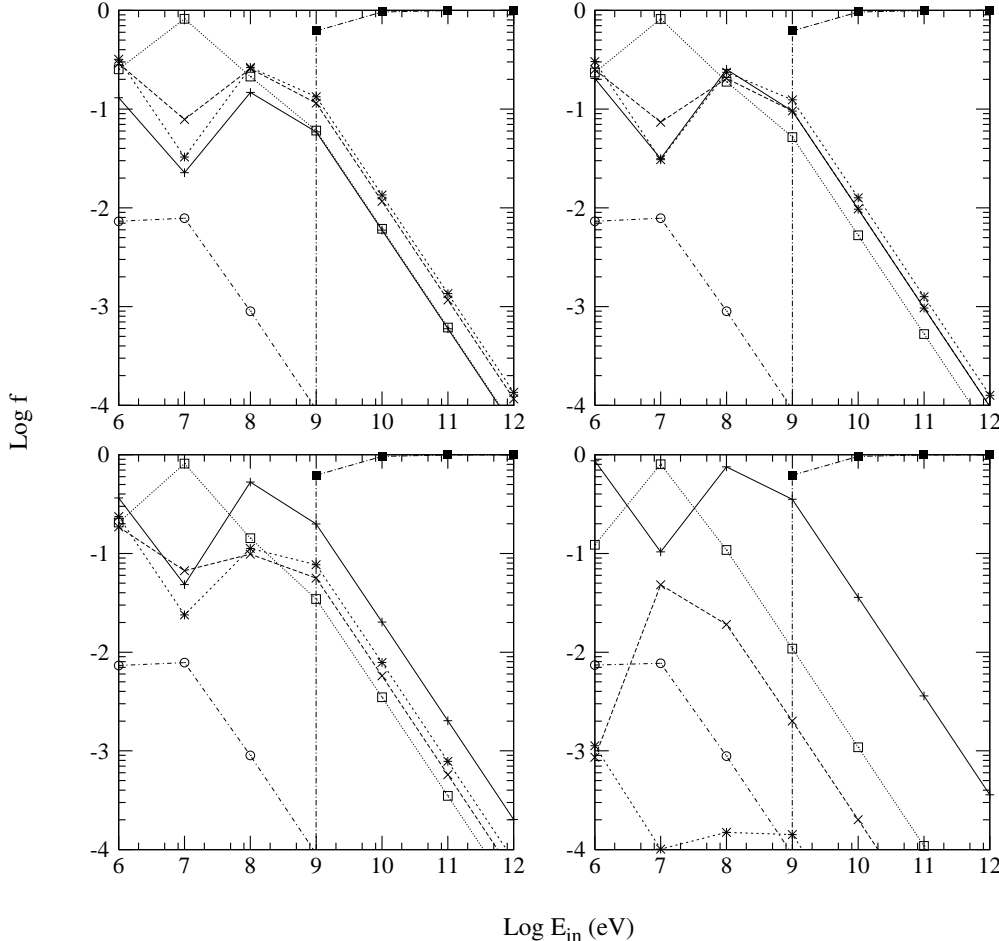


Figure 5. Fractional energy losses as a function of initial electron energy at $z = 10$ for $x_e = 1.000 \cdot 10^{-4}$, $2.147 \cdot 10^{-3}$, $4.610 \cdot 10^{-2}$, $9.900 \cdot 10^{-1}$ left to right, top to bottom panels. The data points as in Fig 4 stand for: photons with $E < 10.2\text{ eV}$ (squares); gas heating (pluses); Ly α photons (crosses); ionizations (asterisks); high energy photons with $h\nu > 10^4\text{ eV}$ (filled squares); energy of upscattered CMB photons (circles).

ready dominant but is unable to upscatter CMB photons to energies higher than 10.2 eV. These photons, described by f_c , do not interact further with the IGM and therefore almost 80% of the initial electron energy is lost and the values for the remaining fractional energy depositions decrease sharply. As soon as IC preferentially upscatters photons to energies over 13.6 eV f_i rises again. Notice that at $z = 50$ this double peak effect is not present because CMB photons are more energetic and therefore f_c (second line of panels from the bottom) in the range $1\text{ MeV} < E_{\text{in}} < 10\text{ MeV}$ remains higher with respect to the lower z cases.

It is also worth noticing that f_c and f_{HE} are essentially independent from x_e but vary slowly with redshift. Intuitively at higher redshift, when CMB photons have higher energies, the value of f_{HE} grows faster with increasing E_{in} .

In the Appendix A we present the results for a number of MEDEA runs with different parameter choices. The tables report the fractional energy depositions as a function of x_e given a fixed z and E_{in} . Because of the large amount of output data we do not present a complete list of fitting formulae but we refer the reader interested in a particular

application to use the following convenient functional forms as in VF08:

- Fraction f_h of the primary energy deposited into heat:

$$f_h = 1.0 - a(1.0 - x^b) \quad (12)$$

- Fraction f_α of the primary energy converted into Ly α radiation:

$$f_\alpha = a(1.0 - x^b)^c \quad (13)$$

- Fraction f_i of the primary energy deposited into ionizations:

$$f_i = a(1.0 - x^b)^c \quad (14)$$

- Fraction f_c of the primary energy deposited into continuum radiation ($h\nu < 10.2\text{ eV}$):

$$f_c = a(1.0 - x^b)^c \quad (15)$$

where all free parameters depend on the redshift and can be fixed by comparing the functions to their tabulated values in Appendix A.

The fractional energy deposition f_{HE} essentially does not depend on x_e and can be assumed to be constant, while

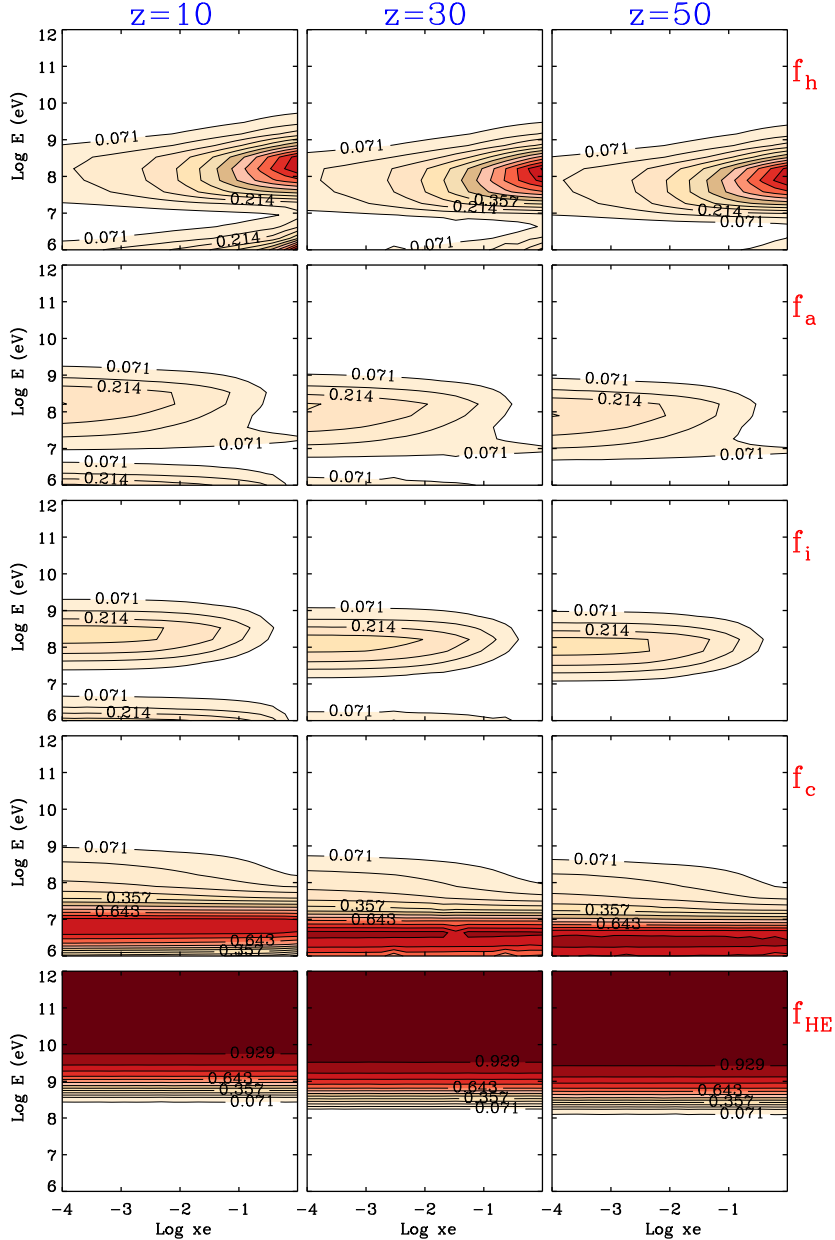


Figure 6. Isocontour plots of the fractional energy depositions as a function of E_{in} and x_e . The panels from top to bottom are relative to f_h , f_a , f_i , f_c , f_{HE} : these are the fraction of the initial electron energy that is deposited into heat, Ly α excitations, ionizations, photons with $E < 10.2$ eV, photons with $E > 10^4$ eV respectively.

f_{CMB} is only reported as a check of energy conservation in every run.

Notice that the errors become smaller for high values of E_{in} until eventually reaching zero in some cases. This is just a natural effect of the calculation and value zero means that the uncertainty becomes smaller than the last significant digit reported in the tables.

4 CONCLUSIONS

We have introduced our code MEDEA, based on a Monte Carlo scheme that makes possible to follow the fate of electrons of energies up to 1 TeV in their secondary energy cas-

cade. Our results represent a substantial generalization of previous works that considered exclusively non-relativistic electrons.

To perform our calculation we implemented in the code a large number of interactions such as collisional ionizations of H, He, HeI; collisional excitations of H, He; electron-electron Coulomb scattering; free-free interactions of electrons with protons; IC with CMB photons; direct collisional excitations to the $2s$ level of HI; indirect cascades from $n \geq 3$ states of HI through the $2s$ level; recombinations. The energy range of the primary electron is $1 \text{ MeV} < E_{\text{in}} < 10 \text{ MeV}$, the ionized fraction considered is $10^{-4} < x_e < 0.99$ and redshift spans $10 < z < 50$.

The results presented here and summarized in numerical form in the Appendix Tables, can be used for many astrophysical applications such as cluster radio relics, DM decays/annihilations, Active Galactic Nuclei, Stellar flares, Gamma Ray Bursts, Pulsar Wind Nebulae, Supernova Remnants and, more generally, whenever it is necessary to deal with the interaction of energetic and/or relativistic particles with the surrounding thermal gas.

We will present new results and updates at the URL <http://www.arcetri.astro.it/twiki/bin/view/DAVID/MedeaCode> periodically.

ACKNOWLEDGMENTS

We thank Naoki Yoshida for his useful suggestions and Steven Furlanetto for insightful comments. This work was supported in part by the Japan Society for the Promotion of Science (JSPS) Postdoctoral Fellowship For Foreign Researchers, Grant-in-Aid for Scientific Research (08804) and by the World Premier International Research Center Initiative (WPI Program).

REFERENCES

- Berg M., Edsjö J., Gondolo P., Lundström E. & Sjörs S., 2009, *JCAP*, 08, 035B
 Blumenthal G. R. & Gould R. J., 1970, *RvMP*, 42, 237B
 Bransden B. H. & Noble C. J., 1976, *J. Phys. B*, 9, 1507
 Chen C. R., Takahashi F. & Yanagida T., 2009, *PhLB*, 673, 255C
 Chuzhoy L. & Shapiro P. R., 2007, *ApJ*, 655, 843C
 Cirelli M., Franceschini R. & Strumia A., 2008, *Nucl. Phys. B*, 800, 204
 Colafrancesco S. & Mele B., 2001, *ApJ*, 562, 24C
 Colafrancesco S., 2004, *A&A*, 422L, 23C
 Colafrancesco S., Profumo S. & Ullio P., 2006, *A&A*, 455, 21
 Dalgarno A., Min Y. & Weihong L., 1999, *ApJS*, 125, 237D
 Ferrari C., 2009, *AIPC*, 1126, 277F
 Furlanetto S. R. & Johnson Stoever S., 2009, arXiv:0910.4410
 Furlanetto S. R., Oh S. P. & Pierpaoli E., 2006, *PhRvD*, 74j, 3502
 Fusco-Femiano R., Landi R. & Orlandini M., 2007, *ApJL*, 654, L9
 Hansen S. H. & Haiman Z., 2004, *ApJ*, 600, 26H
 He X.-G., 2009, arXiv:0908.2908 [hep-ph]
 Hirata C. M., 2006, *MNRAS*, 367, 259
 Hooper D. & Tait T. M. P., 2009, arXiv:0906.0362 [hep-ph]
 Lavalle J., Boehm C. & Barthes J., 2009, arXiv:0907.5589
 Karzas W. J. & Latter R., 1961, *ApJS*, 6, 167
 Kassim N. E., Lazio T. J. W., Ray P.S., Crane P. C., Hicks B. C., Stewart K. P., Cohen A. S., & Lane W.M. 2004, *Planet. Space Sci.*, 52, 1343
 Kim Y.-K. & Rudd M. E., 1994, *Phys. Rev. A*, 50, 3954.
 Koch H. W. & Motz J. W., 1959, *RvMP*, 31, 920K
 Liu J., Yuan Q., Bi X., Li H. & Zhang X., 2009, arXiv:0906.3858
 MacKinnon A. & Mallik P., 2009, arXiv:0908.3903M
 Natarajan A. & Schwarz D., 2009, *PhRvD*, 80d, 3529N
 Peterson J. B., Pen U. L., Wu X. P., 2005, in Kassim N. E., Perez M. R., Junor W., Henning P. A., eds, *ASP Conf. Ser.* Vol. 345, *Searching for Early Ionization with the Primeval Structure Telescope*. Astron. Soc. Pac., San Francisco, p. 441
 Petruk O., 2009, *A&A*, 499, 643P
 Rephaeli Y., 1977, *ApJ*, 212, 608R
 Rephaeli Y., Nevalainen J., Ohashi T. & Bykov A. M., 2008, *Space Science Reviews* 134, 71R
 Resmi L. & Bhattacharya D., 2008, *MNRAS*, 388, 144R
 Shah M. B., Elliot D. S., McCallion P. & Gilbody H. B. , 1988, *J. Phys. B*, 21, 2751
 Shah M. B., Elliot D. S. & Gilbody H. B. , 1987, *J. Phys. B*, 20, 3501
 Shchekinov Y. A. & Vasiliev E. O., 2007, *MNRAS*, 379, 1003S
 Shull J. M., 1979, *ApJ*, 234, 761
 Shull J. M. & van Steenberg M. E., 1985, *ApJ*, 298, 268
 Slatyer T.R., Padmanabhan N. & Finkbeiner D. P., 2009, *PhRvD*, 80d, 3526S
 Spergel D. et al., 2007, *ApJS*, 170, 377S
 Spitzer L., 1962, *Physics of Fully Ionized Gases*, New York: Interscience (2nd edition)
 Spitzer L. & Scott E. H., 1969, *Ap. J.*, 158, 161
 Stone P. M., Kim Y. K. & Desclaux J. P., 2002, *J. Res. Natl. Stand. Technol.*, 107, 327
 The Planck Collaboration, 2006, arXiv:astro-ph/0604069
 Valdés M., Ferrara A., Mapelli M. & Ripamonti, E., 2007, *MNRAS*, 377, 245V
 Valdés M. & Ferrara A., 2008, *MNRAS*, 387L, 8V
 Venter C. & de Jager O. C., 2008, *AIPC*, 1085, 277V
 Wootten A. & Thompson A. R., 2009, arXiv:0904.3739
 Wyithe J. S., Loeb A., Barnes D., 2005, *ApJ*, 634, 715
 Zdziarski A. A. & Svensson R., 1989, *ApJ*, 344, 551

APPENDIX A: TABULATED RESULTS FOR Z=10, 30, 50

In this appendix we present the tabulated results from several of our MEDEA runs in which we fix z and E_{in} and vary the values of the ionized fraction x_e from 10^{-4} to 0.99.

x_e (ionized fraction)	Gas Heating	Excitations (Lyman- α)	Ionizations (H, He, HeII)	Excitations ($E < 10.2$ eV)	HE photons ($E > 10$ keV)	Energy from CMB
1.000e-04	1.3042e-01±5e-04	2.9008e-01±7e-04	3.1945e-01±8e-04	2.5296e-01±7e-04	0.0000e-00±0e-00	7.3151e-03±1e-05
2.779e-04	1.5004e-01±4e-04	2.7835e-01±2e-03	3.1702e-01±2e-03	2.4749e-01±2e-04	0.0000e-00±0e-00	7.2790e-03±7e-05
7.725e-04	1.7376e-01±1e-03	2.6586e-01±2e-03	3.1202e-01±1e-03	2.4126e-01±1e-03	0.0000e-00±0e-00	7.2688e-03±6e-05
2.147e-03	2.0427e-01±1e-03	2.5082e-01±1e-03	3.0280e-01±1e-03	2.3493e-01±1e-03	0.0000e-00±0e-00	7.3067e-03±2e-05
5.968e-03	2.4545e-01±5e-04	2.3235e-01±1e-03	2.8824e-01±1e-03	2.2678e-01±6e-04	0.0000e-00±0e-00	7.2973e-03±1e-05
1.658e-02	2.9845e-01±2e-03	2.1149e-01±1e-03	2.6623e-01±1e-03	2.1657e-01±9e-04	0.0000e-00±0e-00	7.3044e-03±1e-05
4.610e-02	3.6502e-01±1e-03	1.8574e-01±8e-04	2.3621e-01±1e-03	2.0574e-01±9e-04	0.0000e-00±0e-00	7.3117e-03±4e-05
1.281e-01	4.7142e-01±8e-03	1.4661e-01±3e-03	1.8631e-01±3e-03	1.8834e-01±1e-03	0.0000e-00±0e-00	7.3315e-03±0e-00
3.561e-01	6.3845e-01±2e-02	8.9128e-02±9e-03	1.1313e-01±1e-02	1.5249e-01±1e-02	0.0000e-00±0e-00	6.7952e-03±1e-03
9.900e-01	8.6832e-01±1e-04	8.5926e-04±7e-05	1.1260e-03±7e-05	1.2230e-01±4e-05	0.0000e-00±0e-00	7.3883e-03±0e-00

Table A1. Fraction of the energy E_{in} of a 1 MeV primary electron that is deposited into heat, ionizations, Ly α line radiation, photons with energy $E < 10.2$ eV, photons with energies $E > 10$ keV due to Inverse Compton. The last column shows the total energy from the CMB photons before they were upscattered as a test of energy conservation. We consider here redshift $z = 10$.

x_e (ionized fraction)	Gas Heating	Excitations (Lyman- α)	Ionizations (H, He, HeII)	Excitations ($E < 10.2$ eV)	HE photons ($E > 10$ keV)	Energy from CMB
1.000e-04	2.2719e-02±2e-04	7.8486e-02±4e-04	3.2693e-02±6e-04	8.1969e-01±1e-03	0.0000e-00±0e-00	7.8553e-03±3e-05
2.779e-04	2.5005e-02±1e-04	7.6755e-02±2e-04	3.2122e-02±1e-04	8.1969e-01±3e-04	0.0000e-00±0e-00	7.8756e-03±0e-00
7.725e-04	2.7974e-02±1e-04	7.5307e-02±4e-04	3.1826e-02±1e-04	8.1854e-01±5e-04	0.0000e-00±0e-00	7.8607e-03±1e-05
2.147e-03	3.1428e-02±1e-04	7.3635e-02±2e-04	3.0723e-02±1e-04	8.1775e-01±2e-04	0.0000e-00±0e-00	7.8636e-03±1e-05
5.968e-03	3.5781e-02±5e-04	7.1812e-02±4e-04	2.9210e-02±2e-04	8.1690e-01±1e-03	0.0000e-00±0e-00	7.8469e-03±5e-05
1.658e-02	4.1173e-02±1e-04	6.9448e-02±9e-05	2.6939e-02±5e-05	8.1597e-01±1e-04	0.0000e-00±0e-00	7.8704e-03±0e-00
4.610e-02	4.8401e-02±9e-04	6.6941e-02±5e-04	2.3878e-02±4e-04	8.1438e-01±1e-03	0.0000e-00±0e-00	7.8214e-03±1e-04
1.281e-01	5.8480e-02±7e-04	6.2816e-02±5e-04	1.8917e-02±2e-04	8.1332e-01±2e-04	0.0000e-00±0e-00	7.8741e-03±0e-00
3.561e-01	7.5130e-02±1e-03	5.6736e-02±6e-04	1.1091e-02±6e-04	8.1061e-01±5e-04	0.0000e-00±0e-00	7.8853e-03±0e-00
9.900e-01	1.0380e-01±8e-03	4.8136e-02±2e-04	1.0091e-04±1e-05	8.0172e-01±8e-03	0.0000e-00±0e-00	7.7063e-03±2e-04

Table A2. Same as table A1 but for energy $E_{\text{in}} = 10$ MeV.

x_e (ionized fraction)	Gas Heating	Excitations (Lyman- α)	Ionizations (H, He, HeII)	Excitations ($E < 10.2$ eV)	HE photons ($E > 10$ keV)	Energy from CMB
1.000e-04	1.4748e-01±7e-05	2.5673e-01±1e-04	2.6408e-01±1e-04	2.1349e-01±8e-05	0.0000e-00±0e-00	8.9852e-04±0e-00
2.779e-04	1.7047e-01±5e-05	2.4354e-01±1e-04	2.6018e-01±1e-04	2.0753e-01±9e-05	0.0000e-00±0e-00	8.9666e-04±0e-00
7.725e-04	2.0363e-01±8e-05	2.2647e-01±1e-04	2.5193e-01±1e-04	1.9978e-01±1e-04	0.0000e-00±0e-00	8.9668e-04±0e-00
2.147e-03	2.5220e-01±1e-04	2.0427e-01±2e-04	2.3621e-01±2e-04	1.8928e-01±5e-04	0.0000e-00±0e-00	8.9712e-04±0e-00
5.968e-03	3.2200e-01±1e-04	1.7515e-01±1e-04	2.0818e-01±1e-04	1.7646e-01±8e-05	0.0000e-00±0e-00	8.9806e-04±0e-00
1.658e-02	4.1623e-01±1e-04	1.3907e-01±1e-04	1.6585e-01±1e-04	1.6051e-01±6e-05	0.0000e-00±0e-00	8.9863e-04±0e-00
4.610e-02	5.2806e-01±7e-05	9.8462e-02±8e-05	1.1235e-01±8e-05	1.4282e-01±8e-05	0.0000e-00±0e-00	8.9781e-04±0e-00
1.281e-01	6.3468e-01±1e-04	6.0682e-02±5e-05	5.9844e-02±6e-05	1.2647e-01±2e-04	0.0000e-00±0e-00	8.9363e-04±1e-05
3.561e-01	7.1102e-01±4e-05	3.3984e-02±8e-05	2.1616e-02±6e-05	1.1500e-01±1e-04	0.0000e-00±0e-00	8.9426e-04±1e-05
9.900e-01	7.5398e-01±3e-04	1.9103e-02±3e-05	1.4946e-04±0e-00	1.0848e-01±4e-04	0.0000e-00±0e-00	8.8537e-04±2e-05

Table A3. Same as table A1 but for energy $E_{\text{in}} = 100$ MeV.

x_e (ionized fraction)	Gas Heating	Excitations (Lyman- α)	Ionizations (H, He, HeII)	Excitations ($E < 10.2$ eV)	HE photons ($E > 10$ keV)	Energy from CMB
1.000e-04	5.8745e-02±1e-04	1.1476e-01±2e-04	1.3340e-01±3e-04	6.0638e-02±1e-04	6.1871e-01±8e-04	9.0828e-05±0e-00
2.779e-04	6.7436e-02±2e-04	1.0939e-01±3e-04	1.3194e-01±4e-04	5.8250e-02±1e-04	6.1924e-01±1e-03	9.1010e-05±0e-00
7.725e-04	7.9248e-02±1e-04	1.0337e-01±2e-04	1.2943e-01±3e-04	5.5519e-02±1e-04	6.1867e-01±8e-04	9.1025e-05±0e-00
2.147e-03	9.5438e-02±1e-04	9.5723e-02±1e-04	1.2410e-01±1e-04	5.2018e-02±6e-05	6.1898e-01±5e-04	9.1020e-05±0e-00
5.968e-03	1.1865e-01±2e-04	8.6119e-02±1e-04	1.1495e-01±1e-04	4.7679e-02±6e-05	6.1883e-01±6e-04	9.0949e-05±0e-00
1.658e-02	1.5150e-01±2e-04	7.3118e-02±1e-04	9.9394e-02±2e-04	4.1908e-02±6e-05	6.2029e-01±7e-04	9.0998e-05±0e-00
4.610e-02	1.9905e-01±4e-04	5.6280e-02±1e-04	7.6884e-02±2e-04	3.4537e-02±8e-05	6.1945e-01±9e-04	9.0639e-05±0e-00
1.281e-01	2.5848e-01±4e-04	3.5535e-02±8e-05	4.7792e-02±1e-04	2.5526e-02±3e-05	6.1886e-01±6e-04	9.1055e-05±0e-00
3.561e-01	3.1456e-01±7e-04	1.5581e-02±4e-05	1.9543e-02±6e-05	1.6829e-02±3e-05	6.1967e-01±8e-04	9.0561e-05±0e-00
9.900e-01	3.5383e-01±5e-04	2.0031e-03±0e-00	1.4197e-04±0e-00	1.0883e-02±1e-05	6.1933e-01±5e-04	8.9216e-05±0e-00

Table A4. Same as table A1 but for energy $E_{\text{in}} = 1$ GeV.

x_e (ionized fraction)	Gas Heating	Excitations (Lyman- α)	Ionizations (H, He, HeII)	Excitations ($E < 10.2$ eV)	HE photons ($E > 10$ keV)	Energy from CMB
1.000e-04	5.9462e-03±2e-05	1.1624e-02±4e-05	1.3514e-02±5e-05	6.1291e-03±2e-05	9.6141e-01±1e-04	9.1150e-06±0e-00
2.779e-04	6.8388e-03±2e-05	1.1103e-02±3e-05	1.3394e-02±4e-05	5.8970e-03±1e-05	9.6139e-01±1e-04	9.0818e-06±0e-00
7.725e-04	8.0239e-03±1e-05	1.0471e-02±2e-05	1.3119e-02±3e-05	5.6112e-03±1e-05	9.6140e-01±9e-05	9.1103e-06±0e-00
2.147e-03	9.6907e-03±2e-05	9.7353e-03±2e-05	1.2629e-02±4e-05	5.2745e-03±1e-05	9.6129e-01±1e-04	9.1165e-06±0e-00
5.968e-03	1.2006e-02±1e-05	8.7330e-03±1e-05	1.1658e-02±1e-05	4.8212e-03±0e-00	9.6140e-01±4e-05	9.1141e-06±0e-00
1.658e-02	1.5348e-02±2e-05	7.4298e-03±1e-05	1.0100e-02±1e-05	4.2429e-03±0e-00	9.6150e-01±6e-05	9.1052e-06±0e-00
4.610e-02	2.0207e-02±3e-05	5.7406e-03±1e-05	7.8432e-03±1e-05	3.4864e-03±3e-05	9.6134e-01±6e-05	9.2516e-06±0e-00
1.281e-01	2.6227e-02±8e-05	3.6150e-03±1e-05	4.8683e-03±2e-05	2.5793e-03±0e-00	9.6132e-01±1e-04	9.1122e-06±0e-00
3.561e-01	3.1949e-02±6e-05	1.5881e-03±0e-00	1.9956e-03±0e-00	1.6912e-03±0e-00	9.6139e-01±7e-05	9.0471e-06±0e-00
9.900e-01	3.5922e-02±5e-05	2.0074e-04±0e-00	1.4512e-05±0e-00	1.0864e-03±0e-00	9.6139e-01±4e-05	9.0136e-06±0e-00

Table A5. Same as table A1 but for energy $E_{\text{in}} = 10$ GeV.

x_e (ionized fraction)	Gas Heating	Excitations (Lyman- α)	Ionizations (H, He, HeII)	Excitations ($E < 10.2$ eV)	HE photons ($E > 10$ keV)	Energy from CMB
1.000e-04	5.9639e-04±0e-00	1.1654e-03±0e-00	1.3556e-03±0e-00	6.1424e-04±0e-00	9.9613e-01±0e-00	9.0855e-07±0e-00
2.779e-04	6.8470e-04±0e-00	1.1117e-03±0e-00	1.3414e-03±0e-00	5.9045e-04±0e-00	9.9613e-01±0e-00	9.1100e-07±0e-00
7.725e-04	8.0140e-04±0e-00	1.0457e-03±0e-00	1.3100e-03±0e-00	5.6057e-04±0e-00	9.9614e-01±0e-00	9.1199e-07±0e-00
2.147e-03	9.6794e-04±0e-00	9.7279e-04±0e-00	1.2610e-03±0e-00	5.2704e-04±0e-00	9.9613e-01±0e-00	9.1070e-07±0e-00
5.968e-03	1.2015e-03±0e-00	8.7412e-04±0e-00	1.1669e-03±0e-00	4.8255e-04±0e-00	9.9613e-01±0e-00	9.1039e-07±0e-00
1.658e-02	1.5374e-03±0e-00	7.4403e-04±0e-00	1.0119e-03±0e-00	4.2480e-04±0e-00	9.9614e-01±0e-00	9.1118e-07±0e-00
4.610e-02	2.0177e-03±0e-00	5.7279e-04±0e-00	7.8245e-04±0e-00	3.4990e-04±0e-00	9.9613e-01±1e-05	9.1113e-07±0e-00
1.281e-01	2.6192e-03±0e-00	3.6098e-04±0e-00	4.8611e-04±0e-00	2.5767e-04±0e-00	9.9613e-01±0e-00	9.0617e-07±0e-00
3.561e-01	3.1890e-03±1e-05	1.5844e-04±0e-00	1.9910e-04±0e-00	1.6954e-04±0e-00	9.9614e-01±1e-05	9.1139e-07±0e-00
9.900e-01	3.5979e-03±0e-00	2.0092e-05±0e-00	1.4512e-06±0e-00	1.0892e-04±0e-00	9.9613e-01±0e-00	8.9809e-07±0e-00

Table A6. Same as table A1 but for energy $E_{\text{in}} = 100$ GeV.

x_e (ionized fraction)	Gas Heating	Excitations (Lyman- α)	Ionizations (H, He, HeII)	Excitations ($E < 10.2$ eV)	HE photons ($E > 10$ keV)	Energy from CMB
1.000e-04	5.9519e-05±0e-00	1.1637e-04±0e-00	1.3531e-04±0e-00	6.1362e-05±0e-00	9.9961e-01±0e-00	9.1146e-08±0e-00
2.779e-04	6.8263e-05±0e-00	1.1079e-04±0e-00	1.3369e-04±0e-00	5.8872e-05±0e-00	9.9961e-01±0e-00	9.1021e-08±0e-00
7.725e-04	8.0141e-05±0e-00	1.0461e-04±0e-00	1.3102e-04±0e-00	5.6055e-05±0e-00	9.9961e-01±0e-00	9.1010e-08±0e-00
2.147e-03	9.6919e-05±0e-00	9.7361e-05±0e-00	1.2628e-04±0e-00	5.2744e-05±0e-00	9.9961e-01±0e-00	9.1096e-08±0e-00
5.968e-03	1.2010e-04±0e-00	8.7357e-05±0e-00	1.1660e-04±0e-00	4.8193e-05±0e-00	9.9961e-01±0e-00	9.0909e-08±0e-00
1.658e-02	1.5380e-04±0e-00	7.4406e-05±0e-00	1.0123e-04±0e-00	4.2479e-05±0e-00	9.9961e-01±0e-00	9.1139e-08±0e-00
4.610e-02	2.0188e-04±0e-00	5.7279e-05±0e-00	7.8283e-05±0e-00	3.4933e-05±0e-00	9.9961e-01±0e-00	8.8266e-08±0e-00
1.281e-01	2.6155e-04±0e-00	3.6048e-05±0e-00	4.8541e-05±0e-00	2.5755e-05±0e-00	9.9961e-01±0e-00	9.1178e-08±0e-00
3.561e-01	3.1947e-04±0e-00	1.5889e-05±0e-00	1.9965e-05±0e-00	1.6965e-05±0e-00	9.9961e-01±0e-00	9.0696e-08±0e-00
9.900e-01	3.5875e-04±0e-00	2.0092e-06±0e-00	1.4461e-07±0e-00	1.0908e-05±0e-00	9.9961e-01±0e-00	9.0716e-08±0e-00

Table A7. Same as table A1 but for energy $E_{\text{in}} = 1$ TeV.

x_e (ionized fraction)	Gas Heating	Excitations (Lyman- α)	Ionizations (H, He, HeII)	Excitations ($E < 10.2$ eV)	HE photons ($E > 10$ keV)	Energy from CMB
1.000e-04	4.7949e-02±7e-04	1.0609e-01±1e-03	1.1792e-01±2e-03	6.6748e-01±3e-03	0.0000e-00±0e-00	6.0649e-02±3e-04
2.779e-04	5.5115e-02±1e-03	1.0305e-01±2e-03	1.1828e-01±2e-03	6.6338e-01±5e-03	0.0000e-00±0e-00	6.0253e-02±6e-04
7.725e-04	6.3611e-02±9e-04	9.7990e-02±2e-03	1.1581e-01±1e-03	6.6220e-01±3e-03	0.0000e-00±0e-00	6.0483e-02±3e-04
2.147e-03	7.4715e-02±2e-03	9.2606e-02±2e-03	1.1272e-01±2e-03	6.5958e-01±5e-03	0.0000e-00±0e-00	6.0460e-02±6e-04
5.968e-03	8.9678e-02±2e-03	8.5730e-02±2e-03	1.0748e-01±2e-03	6.5665e-01±5e-03	0.0000e-00±0e-00	6.0509e-02±6e-04
1.659e-02	1.0838e-01±7e-04	7.6995e-02±3e-04	9.9004e-02±7e-04	6.5495e-01±1e-03	0.0000e-00±0e-00	6.0697e-02±1e-04
4.611e-02	1.3406e-01±3e-03	6.8027e-02±1e-03	8.6996e-02±1e-03	6.5028e-01±2e-03	0.0000e-00±0e-00	6.0671e-02±2e-04
1.281e-01	1.7903e-01±1e-02	5.4899e-02±2e-03	7.0672e-02±2e-03	6.3574e-01±1e-02	0.0000e-00±0e-00	5.9656e-02±1e-03
3.562e-01	2.4571e-01±1e-02	3.0146e-02±2e-03	3.9021e-02±3e-03	6.2525e-01±1e-02	0.0000e-00±0e-00	5.9872e-02±1e-03
9.900e-01	3.2804e-01±2e-02	3.1720e-04±6e-05	3.7808e-04±5e-05	6.1190e-01±2e-02	0.0000e-00±0e-00	5.9360e-02±2e-03

Table A8. Fraction of the energy E_{in} of a 1 MeV primary electron that is deposited into heat, ionizations, Ly α line radiation, photons with energy $E < 10.2$ eV, photons with energies $E > 10$ keV due to Inverse Compton. The last column shows the total energy from the CMB photons before they were upscattered as a test of energy conservation. We consider here redshift $z = 30$.

x_e (ionized fraction)	Gas Heating	Excitations (Lyman- α)	Ionizations (H, He, HeII)	Excitations ($E < 10.2$ eV)	HE photons ($E > 10$ keV)	Energy from CMB
1.000e-04	6.5170e-02±2e-04	1.1944e-01±2e-04	2.6558e-02±2e-04	6.0778e-01±5e-04	0.0000e-00±0e-00	1.3215e-02±4e-05
2.779e-04	7.2613e-02±9e-05	1.1505e-01±2e-04	2.5641e-02±2e-04	6.0580e-01±4e-04	0.0000e-00±0e-00	1.3211e-02±2e-05
7.725e-04	8.2565e-02±2e-04	1.0961e-01±4e-04	2.3998e-02±2e-04	6.0305e-01±5e-04	0.0000e-00±0e-00	1.3209e-02±4e-05
2.147e-03	9.4603e-02±3e-04	1.0328e-01±3e-04	2.0942e-02±5e-04	6.0027e-01±9e-04	0.0000e-00±0e-00	1.3197e-02±8e-05
5.968e-03	1.0687e-01±2e-04	9.7519e-02±3e-04	1.7271e-02±2e-04	5.9751e-01±4e-04	0.0000e-00±0e-00	1.3194e-02±5e-05
1.659e-02	1.1754e-01±3e-04	9.2524e-02±2e-04	1.3634e-02±3e-04	5.9544e-01±7e-04	0.0000e-00±0e-00	1.3193e-02±8e-05
4.611e-02	1.2576e-01±5e-04	8.9044e-02±4e-04	1.0509e-02±3e-04	5.9370e-01±1e-03	0.0000e-00±0e-00	1.3200e-02±8e-05
1.281e-01	1.3280e-01±6e-04	8.6449e-02±4e-04	7.6575e-03±4e-04	5.9231e-01±1e-03	0.0000e-00±0e-00	1.3206e-02±8e-05
3.562e-01	1.4116e-01±2e-03	8.3597e-02±4e-04	4.2616e-03±4e-04	5.9028e-01±2e-03	0.0000e-00±0e-00	1.3106e-02±2e-04
9.900e-01	1.5355e-01±6e-03	8.0184e-02±3e-04	5.1136e-05±1e-05	5.8547e-01±6e-03	0.0000e-00±0e-00	1.3022e-02±2e-04

Table A9. Same as table A8 but for energy $E_{\text{in}} = 10$ MeV.

x_e (ionized fraction)	Gas Heating	Excitations (Lyman- α)	Ionizations (H, He, HeII)	Excitations ($E < 10.2$ eV)	HE photons ($E > 10$ keV)	Energy from CMB
1.000e-04	1.5026e-01±7e-05	2.7986e-01±1e-04	3.1049e-01±1e-04	1.8201e-01±8e-05	1.6601e-04±1e-04	1.4322e-03±0e-00
2.779e-04	1.7274e-01±7e-05	2.6661e-01±1e-04	3.0699e-01±9e-05	1.7611e-01±9e-05	2.9947e-04±1e-04	1.4327e-03±0e-00
7.725e-04	2.0442e-01±1e-04	2.5009e-01±2e-04	2.9964e-01±2e-04	1.6846e-01±5e-04	1.3948e-04±1e-04	1.4301e-03±0e-00
2.147e-03	2.4961e-01±1e-04	2.2910e-01±1e-04	2.8492e-01±1e-04	1.5900e-01±7e-05	2.0441e-04±1e-04	1.4348e-03±0e-00
5.968e-03	3.1527e-01±1e-04	2.0186e-01±1e-04	2.5877e-01±7e-05	1.4669e-01±8e-05	2.3742e-04±1e-04	1.4310e-03±0e-00
1.659e-02	4.0853e-01±1e-04	1.6631e-01±1e-04	2.1675e-01±1e-04	1.3091e-01±8e-05	1.9667e-04±1e-04	1.4290e-03±0e-00
4.611e-02	5.3057e-01±2e-04	1.2215e-01±1e-04	1.5794e-01±1e-04	1.1177e-01±7e-05	2.2250e-04±1e-04	1.4339e-03±0e-00
1.281e-01	6.6513e-01±2e-04	7.4742e-02±7e-05	9.1325e-02±1e-04	9.1234e-02±1e-04	2.0928e-04±2e-04	1.4275e-03±0e-00
3.562e-01	7.7729e-01±4e-04	3.5669e-02±9e-05	3.5254e-02±7e-05	7.4237e-02±4e-04	1.8391e-04±1e-04	1.4207e-03±2e-05
9.900e-01	8.4660e-01±2e-04	1.1518e-02±3e-05	2.4533e-04±0e-00	6.3929e-02±3e-04	3.6417e-04±2e-04	1.4242e-03±3e-05

Table A10. Same as table A8 but for energy $E_{\text{in}} = 100$ MeV.

x_e (ionized fraction)	Gas Heating	Excitations (Lyman- α)	Ionizations (H, He, HeII)	Excitations ($E < 10.2$ eV)	HE photons ($E > 10$ keV)	Energy from CMB
1.000e-04	3.4982e-02±1e-04	6.9174e-02±3e-04	8.0259e-02±3e-04	3.6397e-02±1e-04	7.7092e-01±9e-04	1.4423e-04±0e-00
2.779e-04	4.0132e-02±1e-04	6.6110e-02±2e-04	7.9542e-02±3e-04	3.5038e-02±1e-04	7.7090e-01±8e-04	1.4438e-04±0e-00
7.725e-04	4.6999e-02±2e-04	6.2419e-02±3e-04	7.7974e-02±4e-04	3.3367e-02±1e-04	7.7096e-01±1e-03	1.4452e-04±0e-00
2.147e-03	5.6658e-02±1e-04	5.8146e-02±2e-04	7.5226e-02±2e-04	3.1410e-02±7e-05	7.7030e-01±6e-04	1.4378e-04±0e-00
5.968e-03	6.9999e-02±2e-04	5.2293e-02±2e-04	6.9671e-02±2e-04	2.8754e-02±8e-05	7.7101e-01±6e-04	1.4367e-04±0e-00
1.659e-02	8.9393e-02±2e-04	4.4778e-02±1e-04	6.0818e-02±1e-04	2.5424e-02±4e-05	7.7129e-01±5e-04	1.4431e-04±0e-00
4.611e-02	1.1757e-01±4e-04	3.4888e-02±1e-04	4.7676e-02±2e-04	2.1098e-02±6e-05	7.7046e-01±8e-04	1.4457e-04±0e-00
1.281e-01	1.5299e-01±3e-04	2.2289e-02±7e-05	3.0077e-02±9e-05	1.5611e-02±3e-05	7.7071e-01±5e-04	1.4451e-04±0e-00
3.562e-01	1.8792e-01±4e-04	9.9416e-03±4e-05	1.2576e-02±4e-05	1.0227e-02±3e-05	7.7102e-01±5e-04	1.4431e-04±0e-00
9.900e-01	2.1305e-01±6e-04	1.1995e-03±0e-00	9.3508e-05±0e-00	6.3982e-03±5e-05	7.7095e-01±6e-04	1.4076e-04±0e-00

Table A11. Same as table A8 but for energy $E_{\text{in}} = 1$ GeV.

x_e (ionized fraction)	Gas Heating	Excitations (Lyman- α)	Ionizations (H, He, HeII)	Excitations ($E < 10.2$ eV)	HE photons ($E > 10$ keV)	Energy from CMB
1.000e-04	3.5042e-03±1e-05	6.9298e-03±3e-05	8.0414e-03±3e-05	3.6454e-03±1e-05	9.7705e-01±9e-05	1.4436e-05±0e-00
2.779e-04	4.0274e-03±1e-05	6.6343e-03±2e-05	7.9838e-03±3e-05	3.5137e-03±0e-00	9.7701e-01±7e-05	1.4419e-05±0e-00
7.725e-04	4.7147e-03±0e-00	6.2647e-03±1e-05	7.8255e-03±2e-05	3.3466e-03±0e-00	9.7702e-01±5e-05	1.4435e-05±0e-00
2.147e-03	5.6701e-03±1e-05	5.8218e-03±2e-05	7.5302e-03±2e-05	3.1443e-03±0e-00	9.7701e-01±6e-05	1.4418e-05±0e-00
5.968e-03	7.0342e-03±2e-05	5.2585e-03±2e-05	7.0073e-03±2e-05	2.8888e-03±0e-00	9.7698e-01±6e-05	1.4414e-05±0e-00
1.659e-02	8.9826e-03±3e-05	4.5036e-03±2e-05	6.1184e-03±3e-05	2.5537e-03±0e-00	9.7701e-01±9e-05	1.4426e-05±0e-00
4.611e-02	1.1768e-02±2e-05	3.4923e-03±0e-00	4.7737e-03±1e-05	2.1111e-03±0e-00	9.7702e-01±5e-05	1.4440e-05±0e-00
1.281e-01	1.5347e-02±5e-05	2.2383e-03±0e-00	3.0212e-03±1e-05	1.5651e-03±0e-00	9.7700e-01±7e-05	1.4447e-05±0e-00
3.562e-01	1.8853e-02±7e-05	9.9756e-04±0e-00	1.2631e-03±0e-00	1.0237e-03±0e-00	9.7703e-01±9e-05	1.4331e-05±0e-00
9.900e-01	2.1387e-02±4e-05	1.1971e-04±0e-00	9.3111e-06±0e-00	6.3960e-04±0e-00	9.7701e-01±4e-05	1.4214e-05±0e-00

Table A12. Same as table A8 but for energy $E_{\text{in}} = 10$ GeV.

x_e (ionized fraction)	Gas Heating	Excitations (Lyman- α)	Ionizations (H, He, HeII)	Excitations ($E < 10.2$ eV)	HE photons ($E > 10$ keV)	Energy from CMB
1.000e-04	3.5090e-04±0e-00	6.9417e-04±0e-00	8.0536e-04±0e-00	3.6504e-04±0e-00	9.9770e-01±1e-05	1.4428e-06±0e-00
2.779e-04	4.0318e-04±0e-00	6.6436e-04±0e-00	7.9940e-04±0e-00	3.5179e-04±0e-00	9.9770e-01±0e-00	1.4459e-06±0e-00
7.725e-04	4.7170e-04±0e-00	6.2667e-04±0e-00	7.8295e-04±0e-00	3.3443e-04±0e-00	9.9770e-01±0e-00	1.4504e-06±0e-00
2.147e-03	5.6732e-04±0e-00	5.8250e-04±0e-00	7.5359e-04±0e-00	3.1450e-04±0e-00	9.9770e-01±0e-00	1.4379e-06±0e-00
5.968e-03	7.0301e-04±0e-00	5.2560e-04±0e-00	7.0031e-04±0e-00	2.8848e-04±0e-00	9.9770e-01±0e-00	1.4240e-06±0e-00
1.659e-02	8.9763e-04±0e-00	4.4973e-04±0e-00	6.1114e-04±0e-00	2.5509e-04±0e-00	9.9770e-01±0e-00	1.4463e-06±0e-00
4.611e-02	1.1773e-03±0e-00	3.4952e-04±0e-00	4.7774e-04±0e-00	2.1095e-04±0e-00	9.9770e-01±0e-00	1.4110e-06±0e-00
1.281e-01	1.5355e-03±0e-00	2.2404e-04±0e-00	3.0231e-04±0e-00	1.5653e-04±0e-00	9.9770e-01±0e-00	1.4356e-06±0e-00
3.562e-01	1.8874e-03±0e-00	9.9928e-05±0e-00	1.2646e-04±0e-00	1.0260e-04±0e-00	9.9770e-01±0e-00	1.4491e-06±0e-00
9.900e-01	2.1359e-03±0e-00	1.2005e-05±0e-00	9.3136e-07±0e-00	6.4095e-05±0e-00	9.9770e-01±0e-00	1.4297e-06±0e-00

Table A13. Same as table A8 but for energy $E_{\text{in}} = 100$ GeV.

x_e (ionized fraction)	Gas Heating	Excitations (Lyman- α)	Ionizations (H, He, HeII)	Excitations ($E < 10.2$ eV)	HE photons ($E > 10$ keV)	Energy from CMB
1.000e-04	3.5062e-05±0e-00	6.9376e-05±0e-00	8.0463e-05±0e-00	3.6491e-05±0e-00	9.9977e-01±0e-00	1.4450e-07±0e-00
2.779e-04	4.0301e-05±0e-00	6.6415e-05±0e-00	7.9895e-05±0e-00	3.5172e-05±0e-00	9.9977e-01±0e-00	1.4458e-07±0e-00
7.725e-04	4.7208e-05±0e-00	6.2730e-05±0e-00	7.8365e-05±0e-00	3.3504e-05±0e-00	9.9977e-01±0e-00	1.4457e-07±0e-00
2.147e-03	5.6731e-05±0e-00	5.8230e-05±0e-00	7.5355e-05±0e-00	3.1444e-05±0e-00	9.9977e-01±0e-00	1.4372e-07±0e-00
5.968e-03	7.0191e-05±0e-00	5.2465e-05±0e-00	6.9898e-05±0e-00	2.8839e-05±0e-00	9.9977e-01±0e-00	1.4445e-07±0e-00
1.659e-02	8.9687e-05±0e-00	4.4938e-05±0e-00	6.1055e-05±0e-00	2.5490e-05±0e-00	9.9977e-01±0e-00	1.4460e-07±0e-00
4.611e-02	1.1769e-04±0e-00	3.4929e-05±0e-00	4.7759e-05±0e-00	2.1092e-05±0e-00	9.9977e-01±0e-00	1.4348e-07±0e-00
1.281e-01	1.5332e-04±0e-00	2.2360e-05±0e-00	3.0174e-05±0e-00	1.5647e-05±0e-00	9.9977e-01±0e-00	1.4463e-07±0e-00
3.562e-01	1.8862e-04±0e-00	9.9770e-06±0e-00	1.2636e-05±0e-00	1.0248e-05±0e-00	9.9977e-01±0e-00	1.4552e-07±0e-00
9.900e-01	2.1377e-04±0e-00	1.1994e-06±0e-00	9.3606e-08±0e-00	6.4119e-06±0e-00	9.9977e-01±0e-00	1.4344e-07±0e-00

Table A14. Same as table A8 but for energy $E_{\text{in}} = 1$ TeV.

x_e (ionized fraction)	Gas Heating	Excitations (Lyman- α)	Ionizations (H, He, HeII)	Excitations ($E < 10.2$ eV)	HE photons ($E > 10$ keV)	Energy from CMB
1.000e-04	2.1464e-02±6e-04	4.7691e-02±1e-03	5.3596e-02±2e-03	7.8527e-01±3e-03	0.0000e-00±0e-00	9.2015e-02±6e-04
2.779e-04	2.4840e-02±2e-03	4.6612e-02±4e-03	5.3886e-02±5e-03	7.8269e-01±1e-02	0.0000e-00±0e-00	9.1998e-02±1e-03
7.725e-04	2.7823e-02±4e-04	4.2640e-02±7e-04	5.1324e-02±6e-04	7.8573e-01±1e-03	0.0000e-00±0e-00	9.2518e-02±2e-04
2.147e-03	3.3214e-02±7e-04	4.0728e-02±1e-03	5.0252e-02±8e-04	7.8351e-01±2e-03	0.0000e-00±0e-00	9.2312e-02±3e-04
5.968e-03	3.9490e-02±1e-03	3.7864e-02±1e-03	4.7959e-02±1e-03	7.8240e-01±2e-03	0.0000e-00±0e-00	9.2316e-02±4e-04
1.659e-02	4.8279e-02±2e-03	3.4619e-02±1e-03	4.4487e-02±2e-03	7.8042e-01±5e-03	0.0000e-00±0e-00	9.2213e-02±9e-04
4.611e-02	6.0673e-02±3e-03	3.0751e-02±2e-03	4.0295e-02±2e-03	7.7664e-01±6e-03	0.0000e-00±0e-00	9.1642e-02±2e-03
1.281e-01	8.0938e-02±4e-03	2.3972e-02±2e-03	3.1881e-02±2e-03	7.7194e-01±6e-03	0.0000e-00±0e-00	9.1268e-02±1e-03
3.562e-01	1.0719e-01±7e-03	1.3114e-02±7e-04	1.7022e-02±9e-04	7.7065e-01±7e-03	0.0000e-00±0e-00	9.2023e-02±1e-03
9.900e-01	1.7492e-01±3e-02	1.4520e-04±5e-05	1.9040e-04±6e-05	7.3680e-01±3e-02	0.0000e-00±0e-00	8.7949e-02±4e-03

Table A15. Fraction of the energy E_{in} of a 1 MeV primary electron that is deposited into heat, ionizations, Ly α line radiation, photons with energy $E < 10.2$ eV, photons with energies $E > 10$ keV due to Inverse Compton. The last column shows the total energy from the CMB photons before they were upscattered as a test of energy conservation. We consider here redshift $z = 50$.

x_e (ionized fraction)	Gas Heating	Excitations (Lyman- α)	Ionizations (H, He, HeII)	Excitations ($E < 10.2$ eV)	HE photons ($E > 10$ keV)	Energy from CMB
1.000e-04	8.7513e-02±2e-04	1.3675e-01±4e-04	4.1413e-02±3e-04	5.0827e-01±7e-04	0.0000e-00±0e-00	1.6381e-02±8e-05
2.779e-04	9.8787e-02±2e-04	1.3023e-01±5e-04	3.9967e-02±5e-04	5.0524e-01±9e-04	0.0000e-00±0e-00	1.6292e-02±2e-04
7.725e-04	1.1476e-01±2e-04	1.2139e-01±3e-04	3.6426e-02±2e-04	5.0138e-01±6e-04	0.0000e-00±0e-00	1.6366e-02±7e-05
2.147e-03	1.3547e-01±4e-04	1.1109e-01±5e-04	3.1073e-02±3e-04	4.9636e-01±1e-03	0.0000e-00±0e-00	1.6356e-02±1e-04
5.968e-03	1.5874e-01±4e-04	1.0003e-01±3e-04	2.3829e-02±3e-04	4.9143e-01±7e-04	0.0000e-00±0e-00	1.6358e-02±1e-04
1.659e-02	1.8046e-01±5e-04	9.0628e-02±4e-04	1.5941e-02±4e-04	4.8689e-01±1e-03	0.0000e-00±0e-00	1.6332e-02±2e-04
4.611e-02	1.9638e-01±5e-04	8.3771e-02±3e-04	9.5488e-03±3e-04	4.8417e-01±8e-04	0.0000e-00±0e-00	1.6391e-02±9e-05
1.281e-01	2.0678e-01±5e-04	7.9688e-02±3e-04	5.3475e-03±2e-04	4.8205e-01±6e-04	0.0000e-00±0e-00	1.6358e-02±8e-05
3.562e-01	2.1389e-01±9e-04	7.7199e-02±3e-04	2.4317e-03±1e-04	4.8065e-01±1e-03	0.0000e-00±0e-00	1.6262e-02±2e-04
9.900e-01	2.2143e-01±3e-03	7.5084e-02±3e-04	2.1216e-05±0e-00	4.7777e-01±2e-03	0.0000e-00±0e-00	1.5950e-02±4e-04

Table A16. Same as table A15 but for energy $E_{\text{in}} = 10$ MeV.

x_e (ionized fraction)	Gas Heating	Excitations (Lyman- α)	Ionizations (H, He, HeII)	Excitations ($E < 10.2$ eV)	HE photons ($E > 10$ keV)	Energy from CMB
1.000e-04	1.5014e-01±5e-05	2.8695e-01±2e-04	3.2422e-01±1e-04	1.7231e-01±1e-04	3.3436e-03±5e-04	1.7491e-03±0e-00
2.779e-04	1.7239e-01±1e-04	2.7407e-01±2e-04	3.2116e-01±3e-04	1.6658e-01±1e-04	2.7406e-03±7e-04	1.7468e-03±0e-00
7.725e-04	2.0298e-01±2e-04	2.5781e-01±2e-04	3.1410e-01±3e-04	1.5916e-01±2e-04	2.8659e-03±7e-04	1.7452e-03±1e-05
2.147e-03	2.4624e-01±2e-04	2.3739e-01±2e-04	3.0016e-01±2e-04	1.4987e-01±8e-05	3.3213e-03±5e-04	1.7494e-03±0e-00
5.968e-03	3.0900e-01±2e-04	2.1138e-01±2e-04	2.7551e-01±2e-04	1.3816e-01±1e-04	2.9106e-03±6e-04	1.7525e-03±0e-00
1.659e-02	3.9881e-01±3e-04	1.7692e-01±1e-04	2.3497e-01±2e-04	1.2279e-01±1e-04	3.3355e-03±6e-04	1.7415e-03±2e-05
4.611e-02	5.2105e-01±4e-04	1.3283e-01±2e-04	1.7634e-01±2e-04	1.0361e-01±1e-04	2.9545e-03±5e-04	1.7451e-03±1e-05
1.281e-01	6.6337e-01±4e-04	8.2768e-02±1e-04	1.0590e-01±1e-04	8.1943e-02±1e-04	2.7966e-03±5e-04	1.7449e-03±1e-05
3.562e-01	7.9064e-01±3e-04	3.8281e-02±4e-05	4.2318e-02±8e-05	6.2668e-02±7e-05	2.9297e-03±3e-04	1.7313e-03±2e-05
9.900e-01	8.7471e-01±7e-04	9.1588e-03±3e-05	3.0206e-04±0e-00	4.9806e-02±5e-04	2.8655e-03±5e-04	1.7198e-03±3e-05

Table A17. Same as table A15 but for energy $E_{\text{in}} = 100$ MeV.

x_e (ionized fraction)	Gas Heating	Excitations (Lyman- α)	Ionizations (H, He, HeII)	Excitations ($E < 10.2$ eV)	HE photons ($E > 10$ keV)	Energy from CMB
1.000e-04	2.7571e-02±1e-04	5.4869e-02±2e-04	6.3583e-02±2e-04	2.8802e-02±8e-05	8.1858e-01±6e-04	1.7572e-04±0e-00
2.779e-04	3.1566e-02±9e-05	5.2382e-02±2e-04	6.2950e-02±2e-04	2.7704e-02±8e-05	8.1880e-01±5e-04	1.7598e-04±0e-00
7.725e-04	3.7050e-02±2e-04	4.9653e-02±3e-04	6.1947e-02±4e-04	2.6463e-02±1e-04	8.1828e-01±1e-03	1.7542e-04±0e-00
2.147e-03	4.4321e-02±1e-04	4.5970e-02±1e-04	5.9412e-02±2e-04	2.4788e-02±6e-05	8.1892e-01±5e-04	1.7634e-04±0e-00
5.968e-03	5.5067e-02±6e-05	4.1726e-02±7e-05	5.5554e-02±9e-05	2.2863e-02±3e-05	8.1818e-01±2e-04	1.7588e-04±0e-00
1.659e-02	7.0094e-02±2e-04	3.5732e-02±1e-04	4.8510e-02±2e-04	2.0198e-02±6e-05	8.1885e-01±6e-04	1.7644e-04±0e-00
4.611e-02	9.2022e-02±3e-04	2.7938e-02±1e-04	3.8190e-02±2e-04	1.6777e-02±5e-05	8.1844e-01±7e-04	1.7566e-04±0e-00
1.281e-01	1.1988e-01±5e-04	1.7980e-02±1e-04	2.4284e-02±1e-04	1.2442e-02±4e-05	8.1878e-01±8e-04	1.7535e-04±0e-00
3.562e-01	1.4856e-01±5e-04	8.1154e-03±3e-05	1.0324e-02±4e-05	8.1512e-03±2e-05	8.1822e-01±5e-04	1.7523e-04±0e-00
9.900e-01	1.6831e-01±7e-04	9.4852e-04±0e-00	7.6582e-05±0e-00	5.0211e-03±1e-05	8.1901e-01±7e-04	1.7432e-04±0e-00

Table A18. Same as table A15 but for energy $E_{\text{in}} = 1$ GeV.

x_e (ionized fraction)	Gas Heating	Excitations (Lyman- α)	Ionizations (H, He, HeII)	Excitations ($E < 10.2$ eV)	HE photons ($E > 10$ keV)	Energy from CMB
1.000e-04	2.7587e-03±0e-00	5.4925e-03±2e-05	6.3624e-03±2e-05	2.8830e-03±0e-00	9.8184e-01±5e-05	1.7624e-05±0e-00
2.779e-04	3.1693e-03±1e-05	5.2615e-03±2e-05	6.3222e-03±3e-05	2.7809e-03±0e-00	9.8181e-01±7e-05	1.7635e-05±0e-00
7.725e-04	3.7000e-03±2e-05	4.9611e-03±2e-05	6.1873e-03±3e-05	2.6446e-03±1e-05	9.8185e-01±8e-05	1.7632e-05±0e-00
2.147e-03	4.4451e-03±1e-05	4.6130e-03±2e-05	5.9606e-03±2e-05	2.4861e-03±0e-00	9.8184e-01±5e-05	1.7635e-05±0e-00
5.968e-03	5.5048e-03±2e-05	4.1708e-03±2e-05	5.5525e-03±3e-05	2.2847e-03±0e-00	9.8183e-01±7e-05	1.7543e-05±0e-00
1.659e-02	7.0190e-03±3e-05	3.5792e-03±1e-05	4.8620e-03±2e-05	2.0218e-03±0e-00	9.8186e-01±7e-05	1.7487e-05±0e-00
4.611e-02	9.2132e-03±2e-05	2.7984e-03±0e-00	3.8265e-03±0e-00	1.6799e-03±0e-00	9.8182e-01±3e-05	1.7578e-05±0e-00
1.281e-01	1.1999e-02±3e-05	1.8000e-03±0e-00	2.4321e-03±0e-00	1.2448e-03±0e-00	9.8186e-01±5e-05	1.7527e-05±0e-00
3.562e-01	1.4824e-02±5e-05	8.1001e-04±0e-00	1.0296e-03±0e-00	8.1436e-04±0e-00	9.8186e-01±6e-05	1.7550e-05±0e-00
9.900e-01	1.6892e-02±5e-05	9.5038e-05±0e-00	7.6904e-06±0e-00	5.0075e-04±0e-00	9.8184e-01±5e-05	1.7205e-05±0e-00

Table A19. Same as table A15 but for energy $E_{\text{in}} = 10$ GeV.

x_e (ionized fraction)	Gas Heating	Excitations (Lyman- α)	Ionizations (H, He, HeII)	Excitations ($E < 10.2$ eV)	HE photons ($E > 10$ keV)	Energy from CMB
1.000e-04	2.7558e-04±0e-00	5.4850e-04±0e-00	6.3558e-04±0e-00	2.8793e-04±0e-00	9.9819e-01±0e-00	1.7582e-06±0e-00
2.779e-04	3.1645e-04±0e-00	5.2523e-04±0e-00	6.3109e-04±0e-00	2.7758e-04±0e-00	9.9818e-01±0e-00	1.7497e-06±0e-00
7.725e-04	3.7029e-04±0e-00	4.9635e-04±0e-00	6.1930e-04±0e-00	2.6459e-04±0e-00	9.9818e-01±0e-00	1.7645e-06±0e-00
2.147e-03	4.4394e-04±0e-00	4.6070e-04±0e-00	5.9514e-04±0e-00	2.4820e-04±0e-00	9.9819e-01±0e-00	1.7453e-06±0e-00
5.968e-03	5.5019e-04±0e-00	4.1694e-04±0e-00	5.5505e-04±0e-00	2.2838e-04±0e-00	9.9818e-01±0e-00	1.7511e-06±0e-00
1.659e-02	7.0310e-04±0e-00	3.5880e-04±0e-00	4.8717e-04±0e-00	2.0263e-04±0e-00	9.9818e-01±0e-00	1.7601e-06±0e-00
4.611e-02	9.2039e-04±0e-00	2.7953e-04±0e-00	3.8212e-04±0e-00	1.6789e-04±0e-00	9.9818e-01±0e-00	1.7616e-06±0e-00
1.281e-01	1.2018e-03±0e-00	1.8043e-04±0e-00	2.4363e-04±0e-00	1.2460e-04±0e-00	9.9818e-01±0e-00	1.7558e-06±0e-00
3.562e-01	1.4845e-03±0e-00	8.1159e-05±0e-00	1.0314e-04±0e-00	8.1416e-05±0e-00	9.9818e-01±0e-00	1.7420e-06±0e-00
9.900e-01	1.6892e-03±0e-00	9.4977e-06±0e-00	7.7807e-07±0e-00	5.0153e-05±0e-00	9.9818e-01±0e-00	1.7333e-06±0e-00

Table A20. Same as table A15 but for energy $E_{\text{in}} = 100$ GeV.

x_e (ionized fraction)	Gas Heating	Excitations (Lyman- α)	Ionizations (H, He, HeII)	Excitations ($E < 10.2$ eV)	HE photons ($E > 10$ keV)	Energy from CMB
1.000e-04	2.7539e-05±0e-00	5.4811e-05±0e-00	6.3515e-05±0e-00	2.8783e-05±0e-00	9.9982e-01±0e-00	1.7656e-07±0e-00
2.779e-04	3.1624e-05±0e-00	5.2490e-05±0e-00	6.3062e-05±0e-00	2.7749e-05±0e-00	9.9982e-01±0e-00	1.7624e-07±0e-00
7.725e-04	3.7066e-05±0e-00	4.9683e-05±0e-00	6.1980e-05±0e-00	2.6472e-05±0e-00	9.9982e-01±0e-00	1.7556e-07±0e-00
2.147e-03	4.4352e-05±0e-00	4.6031e-05±0e-00	5.9463e-05±0e-00	2.4812e-05±0e-00	9.9982e-01±0e-00	1.7623e-07±0e-00
5.968e-03	5.4933e-05±0e-00	4.1606e-05±0e-00	5.5403e-05±0e-00	2.2807e-05±0e-00	9.9982e-01±0e-00	1.7616e-07±0e-00
1.659e-02	7.0164e-05±0e-00	3.5759e-05±0e-00	4.8579e-05±0e-00	2.0173e-05±0e-00	9.9982e-01±0e-00	1.7780e-07±0e-00
4.611e-02	9.2019e-05±0e-00	2.7930e-05±0e-00	3.8186e-05±0e-00	1.6780e-05±0e-00	9.9982e-01±0e-00	1.7657e-07±0e-00
1.281e-01	1.2000e-04±0e-00	1.7997e-05±0e-00	2.4338e-05±0e-00	1.2456e-05±0e-00	9.9982e-01±0e-00	1.7520e-07±0e-00
3.562e-01	1.4852e-04±0e-00	8.1202e-06±0e-00	1.0313e-05±0e-00	8.1501e-06±0e-00	9.9982e-01±0e-00	1.7474e-07±0e-00
9.900e-01	1.6921e-04±0e-00	9.4711e-07±0e-00	7.6533e-08±0e-00	5.0200e-06±0e-00	9.9982e-01±0e-00	1.7437e-07±0e-00

Table A21. Same as table A15 but for energy $E_{\text{in}} = 1$ TeV.